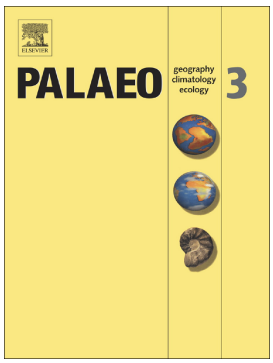

Onset of sedimentation near the Carnian/Norian boundary in the northwestern Sichuan Basin: New evidence from ammonoid biostratigraphy and zircon U-Pb geochronology

Paolo Mietto, Xin Jin, Stefano Manfrin, Gang Lu, Zhiqiang Shi, Piero Gianolla, Xiangtong Huang, Nereo Preto

PII: S0031-0182(21)00031-6

DOI: https://doi.org/10.1016/j.palaeo.2021.110246

Reference: PALAEO 110246

To appear in: *Palaeogeography, Palaeoclimatology, Palaeoecology*

Received date: 22 April 2020

Revised date: 16 January 2021

Accepted date: 17 January 2021

Please cite this article as: P. Mietto, X. Jin, S. Manfrin, et al., Onset of sedimentation near the Carnian/Norian boundary in the northwestern Sichuan Basin: New evidence from ammonoid biostratigraphy and zircon U-Pb geochronology, *Palaeogeography, Palaeoclimatology, Palaeoecology* (2018), https://doi.org/10.1016/j.palaeo.2021.110246

Onset of sedimentation near the Carnian/Norian boundary in the northwestern Sichuan Basin: new evidence from ammonoid biostratigraphy and zircon U-Pb geochronology

Paolo Mietto [1], Xin Jin * [2, 3], Stefano Manfrin [1], Gang Lu [2], Zhiqiang Shi [2], Piero Gianolla [4], Xiangtong Huang [3], Nereo Preto [1]

1. Dipartimento di Geoscienze, Università degli Studi di Padova, Via G. Gradenigo 6, Padova, Italy

2. State Key Laboratory of Oil and Gas Reservoir Geology and Exploitation, Chengdu University of Technology, Chengdu, Sichuan 610059, China

3. State Key Laboratory of Marine Geology, Tongji University, Siping Road, Shanghai, 200092, China

4. Department of Physics and Earth Sciences, Università degli Studi di Ferrara, Via Saragat, 1, Ferrara 44100, Italy

*Corresponding author: jinxin2012cdut@163.com (Xin Jin)

Paolo Mietto: paolo.mietto@unipd.it

stefano.manfrin@regione.veneto.it

Gang Lu: 262346992@qq.com

Zhiqiang Shi: szqcdut@163.com

Piero Gianolla: glr@unife.it

Xiangtong Huang: xiangtong@tongji.edu.cn

Nereo Preto: nereo.preto@unipd.it

Abstract: Upper Triassic deposits formed at the onset of subsidence in the Sichuan foreland Basin of South China, and may record a crisis of carbonate deposition related

to the Carnian Pluvial Episode. However, there is no consensus yet on the precise age of these deposits in northwestern Sichuan. In this work, ammonoid biostratigraphy has been improved, and a U/Pb age from detrital zircons has been obtained from the Upper Triassic of northwestern Sichuan. New ammonoid taxa *Sinotropites sichuanensis* n. gen., n. sp. and *Hadrothisbites hanwangensis* n. sp. are described from the upper part of the Ma'antang Formation in Hanwang and Jushui area and are assigned to the uppermost Tuvalian (*Anatropites spinosus* Zone, *Gonionotites italicus* Subzone). Ammonoid and conodont biostratigraphy, combined with U/Pb concordant ages of 227.2 ± 1.1 Ma (2σ) obtained from youngest detrital zircons, provide a robust constrain on the initial sedimentation phases of the foreland basin in northwestern Sichuan, and suggest that the terrigenous turnover was not related to the Carnian Pluvial Episode.

Keywords: Carnian Pluvial Episode; Ma'antang Formation; Carnian-Norian Boundary; South China

1. Introduction

The Upper Triassic successions of the northwestern Sichuan Basin recorded the onset of subsidence and the beginning of sedimentation in a foreland basin. At the very base of the foreland basin succession, the Ma'antang Formation (Jin et al., 2015, 2018, 2019, 2020; Shi et al., 2019) displays a lithological change from basal oolitic-bioclastic shoals to upper siliceous sponge mounds, then followed by dark grey shales and silty mudstones (Wu, 1989). It has been suggested that carbonate sedimentation

was interrupted by environmental changes associated with a global climate crisis, the "Carnian Pluvial Episode" or CPE (*sensu* Simms and Ruffell, 1989; Shi et al 2017; Dal Corso et al., 2018). Despite the relevance of the Ma'antang Formation for the depositional history of the basin and as a potential record of a major climate crisis, a sharp controversy still remains on its age in the northwestern Sichuan. A rich ammonoid association has been reported in the upper terrigenous facies by Wang (1992), which included late Carnian taxa. Shi et al. (2017) also found ammonoids from this unit, and assigned their specimens to the late Carnian Discotropitidae and Juvavitidae families. Jin et al. (2019) reported one undetermined genus: Tropitidae n. gen., n. sp., and a new species, *Hadrothisbites* n. sp. Ammonoids, conodonts and halobiid bivalves collected by Jin et al. (2019) suggest an age for the Ma'antang Formation in the northwestern Sichuan that is close to the Carnian/Norian boundary, while there is no evidence for the presence of lower Carnian strata. Since the distribution of conodonts and ammonoids does not fully constrain the position of the Carnian/Norian boundary, Jin et al. (2019) proposed two potential positions for the Carnian/Norian boundary at Qingyangou section (HWQ) in Hanwang area, NW Sichuan Basin. The new age model revised substantially the previous age determinations (Zhang et al., 2015; Shi et al., 2017), and excludes that the demise of sponges and the arrival of terrigenous deposits were related to the CPE. The constraints to anchor the Carnian/Norian boundary at HWQ section are unfortunately still loose, as a ca. 12 meter interval with no remarkable fossils is present. Moreover, some ammonoid taxa, i.e., Tropitidae n. gen., n. sp. and *Hadrothisbites* n. sp. have not

yet been described. These uncertainties led Jiang et al. (2019) to re-examine the conodont biostratigraphy of the HWQ section. According to these authors, most of the lower Ma'antang Formation is dated to the early Carnian.

In this paper, we describe the new ammonoid taxa that were anticipated in Jin et al. (2019). Furthermore, we use detrital zircons U/Pb geochronology to constrain the position of the Carnian/Norian boundary at HWQ section, with an absolute age that is fully independent from biostratigraphy. U-Pb ages of detrital zircons are a statistically robust measure for a maximum depositional age (Dickinson and Gehrels, 2009) and are used already to date deposits near the Carnian/Norian boundary in the US (summary in Lucas et al., 2012). With this work, we aim at closing definitively the ongoing controversy on the timing of carbonate crisis in Hanwang area. To this goal, we improved the existing ammonoid biostratigraphy by fully describing those new ammonoid taxa that were still to be formalized, and we used U/Pb geochronology to constrain the Carnian/Norian transition in South China, independently from ammonoid and conodont biostratigraphies, which age significance is still debated.

2. Geological setting

During the Triassic, the Sichuan Basin was a portion of eastern Tethys and was located at the northwestern margin of Yangtze Block (sub-block of the South China Block, Fig. 1A). The basin developed from a Proterozoic-Middle Triassic marine cratonic basin into a Late Triassic-Cenozoic foreland basin (Shi et al., 2019). It was surrounded by the southeastern Jiangnan paleo-land, the northern Qinling-Daba paleo-

land and the southwestern Kangdian paleo-land. The western boundary of the Sichuan Basin was rimmed by the Longmen Shan Thrust Belt (Fig. 1B). Further to the northwest, it is bordered by the Songpan-Ganzi Fold Belt (Fig. 1B), which is considered to be a remnant of the Late Triassic deep oceanic basin (Weislogel et al., 2006). At the end of Middle Triassic, the collision between North China and South China plates resulted in a flexural forebulge unconformity (Zhang et al., 1996; Li et al., 2003, 2014), which brought about an extensive erosion of the Middle Triassic Tianjingshan Formation in most parts of Sichuan Basin and probably prevented the deposition of the lower Carnian, lower part of the overlain Ma'antang Formation in Hanwang area (Jin et al., 2018, 2019). As a consequence of this tectonic activity, the depositional style of the region switched to a Late Triassic foreland basin, the Sichuan Basin, in which deposition continued until Quaternary (Li et al., 2003). In the early Carnian (Late Triassic), the Longmen Shan Thrust Belt was a partly submarine chain connecting the western Sichuan and the Ganzi deep marine basins (Deng et al., 1982; Wu, 1984, 1989). A transgression opened a passage through this chain, then letting waters from the Paleo-Tethys Ocean entering the western Sichuan Basin and forming a semi-enclosed bay (Deng et al., 1982; Wu, 1984, 1989). The local sea level was rising until the early Norian (Li et al., 2014). A Carnian carbonate ramp to basin was formed in front of the Longmen Shan Thrust Belt (Wu, 2009; Li et al., 2014; Jin et al., 2018; Shi et al., 2019). Humid paleo-climate conditions and the foreland basin development accelerated terrigenous clastics input, subsequently triggering the submergence of carbonate platforms in Sichuan Basin under sand and clay sediments (Jin et al., 2018).

3. Material and methods

3.1. Ammonoid preparation

The ammonoids described here were collected in the framework of a previous study (Jin et al., 2019) from two localities (Fig. 1C). One is Qingyangou (HWQ) section (31°27′46.85″N/104°09′35.40″E) and is located at 2 km NW of Hanwang town, northwestern Sichuan Basin. The other is Jushui section (JS) (31°30'30.6"N /104°14'03.56"E), around 9 km apart from HWQ (Fig. 1C and 2). Ammonoids are well preserved, and some of them have been simply described by Jin et al. (2019). Fossils were extracted from rock matrix with needles and consolidated with vinyl glue, then photographed after coating with white MgO powder, except when the suture line was illustrated. All procedures were carried out at the Department of Geosciences, Padova University.

3.2. U-Pb geochronology

One sample (ZQ) of ca. 2 kg was collected from the first fine-grained muddy siltstone layer in the HWQ section (Fig. 2). The siltstone is mainly composed of angular to subangular quartz, pyritized plant tissues, detritus and fine muds. They all are cemented by calcite. The detailed sedimentological characters of the upper terrigenous part have been described, in the nearby Guanyinya section (HWG), by Jin et al. (2015). Detrital zircon grains were first isolated from the sample by combined magnetic and conventional heavy liquid separation and then concentrated by

handpicking at the Langfang Sincerity Geological Service Co., Ltd (Hebei, China). Two hundred and fifty randomly selected grains were mounted in epoxy resin, and sectioned and polished approximately in half to expose the interior parts. Afterwards, transmitted and reflected light images were taken using an optical microscope, and CL images were collected using a JSM-IT100 electron microscope connected to a Gatan MiniCL system at the Wuhan Sample Solution Analytical Technology Co., Ltd., Wuhan. The in-situ U-Pb dating of zircon grains was performed by a LA-ICP-MS at the State Key Laboratory of Marine Geology, Tongji University, China. The laser system was an Agilent 7900 quadrupole ICP-MS coupled to a Resonetics M50 193 nm excimer laser ablation system. The analytical spot was 26 μm in diameter, and the laser energy density was 4 J/cm $^{-2}$, with a frequency of 6 Hz. Zircon standards 91500 (1065.4 ± 0.3 Ma) and Plešovice (337.1 ± 0.4 Ma) (Wiedenbeck et al., 1995; Sláma et al., 2008) were analyzed sequentially with every 10 unknown samples. The data reduction for measured isotopic intensity consists of blank subtraction, isotopic ratio calculation, normalization by the primary zircon isotopic ratios (91500) and instrumental drift correction in a specific sequence. The data reduction, age calculation and uncertainty propagation were performed using the software ICPMSDataCal (Liu et al., 2010). Common Pb correction was conducted following the method of Andersen (2002). The calibrated age data were reported at 1σ level of uncertainty and those for weighted mean ages are given at 2σ level. The weighted mean concordia ages of zircon 91500 (n=14) and Plešovice (n=14) are 1062.3 ± 3.0 Ma and 339.6 ± 1.4 Ma (2σ, standard error), respectively, which are consistent with

the published U-Pb ages (1062 Ma, 337 Ma) within the uncertainty (Wiedenbeck et al., 1995; Sláma et al., 2008).

4. Results

4.1. Ammonoids

The composition of the ammonoid fauna from Qingyingou (HWQ) and Jushui (JS) sections was given in Jin et al. (2019), where a selection of the ammonoid collection was illustrated. Here, we focus on the two new taxa, Tropitidae n. gen., n. sp. and *Hadrothisbites* n. sp., which could not be described in full so far. Tropitidae n. gen., n. sp. is the most common ammonoid in the Upper Triassic of Hanwang and Jushui, while *Hadrothisbites* is a rare genus, that was described so far only from the Tuvalian of the Pardonet Formation of British Columbia (Tozer, 1994). We provide systematic descriptions to facilitate the biostratigraphic correlation, in case these taxa would be found elsewhere, in the paleontological appendix.

4.2. Zircon U/Pb ages

U-Pb isotope analyses were conducted on 130 zircon grains from sample ZQ. One hundred and eight grains yielded concordant ages. The remaining zircons gave discordant ages (discordances >10%) and were excluded from future interpretation. Some zircons gave discordant ages probably as a consequence of Pb-loss, intermediate daughter product disequilibrium and/or mixing of zircon components with different ages during analysis (Schoene, 2014; Reimink et al., 2016). A 10%

level is commonly used to separate the distributions of concordant and discordant data (Spencer et al., 2016). All U-Pb data are presented in the online supplementary data. Most of the zircons were 80 to 150 μm long, with length/width ratios of 1.5 to 3.0, and have rounded or subrounded morphologies (Fig. 3A). Some have fractured margin. The older zircons are commonly characterized by no or unclear cathodoluminescence, while the younger zircons generally show an oscillatory or fan-shaped zoning (Fig. 3A). One hundred and eight analyses plot on or near concordia curve (Fig. 3B). Ages are distributed on a wide range from 225.8 ± 1.4 Ma to 2365.2 ± 15.1 Ma and are grouped into three major age clusters at ca. 225.8 - 461.6 Ma, 580.6 - 1169.1 Ma, 1407.4 - 1885.0 Ma. A minor peak occurs at 2035.3 - 2365.2 Ma (Fig. 3C). The twelve youngest zircon grains yielded concordant ages with a mean age of 227.2 ± 1.1 Ma (2σ, n = 12, Fig. 3D, E).

5. Discussion

The age of the Ma'antang Formation in Hanwang is a matter of debate. Among others, Wu (1989), Zhang et al. (2015), Shi Z-Q et al. (2017) and more recently Jiang et al. (2019) considered the lower, mostly carbonate part of the Ma'antang Formation in Hanwang to have a Julian age (early Carnian). Jin et al. (2018, 2019) instead found evidence that the Tuvalian (upper Carnian) sediments alone was present in Hanwang, the Julian substage being missing, either because of erosion or non-deposition. The disagreement on the age of the Ma'antang Formation still persists, despite the availability of an integrated stratigraphy, which includes upper Tuvalian conodont

assemblage consisting of *Paragondolella noah, Carnepigondolella angulate, Hayashiella tuvalica, Epigondolella miettoi, Carnepigondoella orchard* (Jin et al., 2018); a Julian conodont *Mazzaella carnica* range zone (Jiang et al., 2019); upper Tuvalian ammonoids and Halobiid bivalves, *Hadrothisbites* n. sp., *Gonionotites* sp., *Griesbachites* sp., and *Halobia* cf. *H. septentrionalis* (Jin et al., 2019). Shi et al. (2017) provided new discotropitid genus associated with a conodont species (*Q. polygnathiformis*) with a long range through most of the Carnian. Chemostratigraphy (Jin et al., 2018, 2019) and magnetostratigraphy (Zhang et al., 2015) are also studied in Ma'antang Formation.

A reliable age model for the Ma'antang formation of Hanwang would be a major contribution to understand the evolution of the Sichuan Basin, for which the timing of the initial stages is still poorly constrained (see, e.g., Li et al., 2003). Furthermore, reaching a consensus on the age of the Ma'antang Formation in Hanwang include the Sichuan Basin among the regions providing useful information for the definition of the Carnian/Norian boundary. The new U/Pb age from detrital zircons presented in this work fits into this framework of open scientific questions.

5.1. Zircon U-Pb ages provide a consideration of the Carnian/Norian boundary in Hanwang

So far, there are only a few U-Pb ages linked to solid biostratigraphy (e.g., conodonts and ammonoids) reported in the upper Carnian or lower Norian (Fig. 4). Gehrels et al. (1987) reported an age of 225 ± 3 Ma combined with conodonts from

the Norian of the SE Alaska. Furin et al. (2006) presented a $^{206}Pb/^{238}U$ age of 230.91 ± 0.33 Ma from an ash bed in the upper Carnian of southern Italy. This age determination is so far the most precise with biostratigraphic control near the Carnian/Norian boundary, and, based on conodont and palynomorph biostratigraphy, has to be located in the Tuvalian 1 or 2 (Rigo et al., 2012). More recent studies by Daikow et al. (2012) reported U-Pb ages of 223.8 ± 0.74 and 224.47 ± 0.29 Ma in the middle to upper Norian deposits of British Columbia. Ramezani et al. (2011) obtained zircon ages of ~ 207.79 ± 0.15 to 225.185 ± 0.079 Ma by isotope dilution thermal ionization mass spectrometry (ID-TIMS) from tuffaceous rocks collected at the base and top of the Chinle Formation, respectively, which is thought to span nearly the entire Norian Stage (see also Kent et al., 2018, 2019). Kent et al. (2017) and Maron et al. (2019) gave an age of 227 Ma for the Carnian/Norian boundary basing on magnetostratigraphic correlations of biostratigraphically constrained marine sections of western Tethys with the astrochronological time scale of the Newark Basin. In ZQ sample, the twelve youngest zircon grains have discordances <10% and their mean age is centered at 227.2 ± 1.1 Ma (2σ) (Fig. 3D, E). Dickinson and Gehrels (2009) highlighted that a weighted mean age of the youngest population of zircons (n >3) that overlap in age at 2σ can be a statistically robust measure for a maximum depositional age. This approach has been widely used to pinpoint a single age in several cases (e.g., Ramezani et al., 2011; Langer et al., 2018). We thus propose that the ZQ bed of the HWQ section, at the base of the upper terrigenous part of Ma'antang Formation, is 227.2 ± 1.1 Ma old, or younger. This age is close to the

Carnian/Norian boundary according to Maron et al. (2019), and it is younger than, and does not overlap with, the Tuvalian age of Furin et al. (2006). This implies that the onset of terrigenous deposition and the drowning of sponge reefs in Hanwang are Tuvalian or younger, and most probably close to the base of the Norian, and cannot be related to the onset of the CPE. This U/Pb datation is consistent with the biostratigraphy of Jin et al. (2019). Also, it implies that Julian deposits are not yet documented in the Sichuan Basin of Hanwang. Julian deposits are instead known from other parts of the Sichuan Basin, e.g., at Shiyan village (Ma'antang section reported in Wang, 1992; Shi Z-Q et al., 2019).

5.2. Tropitidae in the Sichuan Basin and the choice of a Norian GSSP

The Global Boundary Section and Point (GSSP) for the base of the Norian is not yet established. A vivid discussion on its placement is ongoing within the Subcommission on Triassic Stratigraphy, and two candidate localities emerged as most likely sections for the Norian GSSP (e.g., Balini et al., 2015): Pizzo Mondello in Sicily, Italy (e.g., Nicora et al., 2007; Balini et al., 2012) and Black Bear Ridge in Canada (Orchard, 2007). The Sichuan Basin was much afar from both of these localities in the Triassic. It lacks some of the characteristics that would be required to be considered as a GSSP (Salvador, 1994): the succession begins with an uncomformity between the Middle and Upper Triassic, and minor uncomformities may occur within the Upper Triassic as well; the fossil content is not as abundant as in other localities, and, for what the ammonoids are concerned, the most common taxon

(*Sinotropites sichuanensis*) was found so far only in the Sichuan Basin. Nevertheless, there is little documentation of the Carnian/Norian boundary in South China, and this makes the record of the Sichuan Basin an important reference for paleogeographic studies and global correlations within this time interval (Jin et al., 2019).

The current discussion on the Norian GSSP is also about the main stratigraphic marker which should be used to best approximate the GSSP. McRoberts and Krystyn (2011) proposed the first appearance of the bivalve *Halobia austriaca* as primary marker for the base of the Norian stage, while Nicora et al. (2007), Orchard (2007) and Mazza et al. (2018) proposed instead the first appearance of conodont *Metapolygnatus parvus*. Other conodont bioevents were put forward as primary markers, albeit less formally than the first occurrence of *M. parvus*. All bioevents are being considered because they occur in between "Carnian" ammonoid faunas (*Anatropites* sp., or the ammonoid associations of the *macrolobatus* Vs *spinosus* ammonoid biozones) and "Norian" ammonoids belonging to genera *Guembelites* and *Dimorphites* (see discussions in, e.g., Balini et al., 2012; Mazza et al., 2018; Orchard, 2019). This is a natural consequence of the historical use of ammonoids to define the Triassic stages (e.g., Tozer, 1994). Since the definition of a GSSP should also "*take account of historical priority and usage and should approximate traditional boundaries*" (Salomon, 1994), in Triassic stratigraphy the reference to ammonoid biostratigraphy is unavoidable.

Overall, the bio-horizons presently considered as potential markers for the base of the Norian occur in an interval of less than 20 m at Pizzo Mondello, which is

centered about the PM4r reverse polarity interval. This reverse polarity interval may be correlated either to the HQ2r, or the HQ4r intervals in HWQ section (corresponding to options A and B in Jin et al., 2019; the nomenclature of magnetic intervals is derived from Muttoni et al., 2004, and Zhang et al., 2015).

The ammonoid record of the Sichuan Basin raises questions about the distribution of Tropitidae. The family Tropitidae includes ammonoids with an ammonitic suture line and often with distinctive morphologies. *Tropites*, the type genus of the family, has a cadicone shell with deep umbilicus and a prominent ventral keel bounded by two ventral furrows; the keeled and often bisulcate venter is a common feature of many Tropitidae, and makes many of the ammonoids belonging to this family easy to identify. The family first appears at the Julian/Tuvalian boundary, and becomes essentially extinct before the Norian, thus, it is typical and diagnostic of the upper Carnian (Tuvalian). The occurrence of Tropitidae was one reason why Jin et al. (2019) attributed part of the upper Ma'antang Formation, mostly terrigenous, to the Tuvalian. The age of beds that yielded *Sinotropites sichuanensis* in Hanwang is however very close to, or even overlapping with, the interval within which the Norian GSSP may be located, and *Sinotropites sichuanensis* is a new species, which stratigraphic distribution is still unknown and has to be inferred from independent data (i.e., distribution of co-occurring fossils, magnetostratigraphic correlations and radiometric datations). Given the uncertainties in correlation (Jin et al., 2019) and the error margins of the U/Pb ages of detrital zircons, it cannot be excluded that some specimens of *Sinotropites sichuanensis* may have been collected from beds that would

be eventually placed in the lower Norian. We suggest that in the (hopefully) imminent choice of a GSSP for the Norian stage, some care will be taken in trying to set the boundary above the last occurrence of *Sinotropites sichuanensis* in the Sichuan Basin, in order to maintain the traditional and commonly used concept that all Tropitidae are Carnian. This would require the ambiguity of the magnetostratigraphic correlations (options A or B in Jin et al., 2019) to be resolved, e.g., by denser sampling for ammonoids and/or additional analyses of detrital zircons in the HWQ section, where magnetostratigraphy is available.

6. Conclusions

Two new ammonoids, *Sinotropites sichuanensis* and *Hadrothisbites jushuiensis* are described in this paper, and were found near the Carnian/Norian boundary of the northwestern Sichuan Basin, Yangtze Block. In the process of defining a GSSP for the Norian, beds of the Sichuan Basin with *Sinotropites sichuanensis* may be eventually end up to be Norian, and this would mean that Tropitidae would be the most common ammonoids in the Norian in the NW Sichuan Basin, differently from anywhere else. A fine grained terrigenous bed at the base of the upper (terrigenous) Ma'antang Formation of Qingyangou yielded abundant zircons. The youngest zircons of this bed yielded concordant ages of 227.2 ± 1.1 Ma, that is, coincident within error margins to the age of the proposed position of the Norian GSSP at Pizzo Mondello, southern Italy. This is the first absolute age associated with solid biostratigraphy that constraints the Carnian/Norian boundary in South China, and a first absolute age

estimation of the beginning of sedimentation in the Sichuan foreland Basin. With zircons as young as 227.2 ± 1.1 Ma occurring at the base of the upper terrigenous part of the Ma'antang Formation near Hanwang, it can be excluded that the terrigenous input in this part of the basin was related to the Carnian Pluvial Episode. It implies that lower Carnian sediments cannot be proved yet to have occurred in the northwestern Sichuan Basin, while they were known already for a more eastern sector of the Sichuan Basin, at Ma'antang.

Acknowledgements

We acknowledge Stefano Castelli (University of Padova) for photographing ammonoid pictures. We thank Editor Prof. Thomas Algeo, Prof. Huan Li (Central South University), and two anonymous reviewers and for their constructive comments which greatly improved our manuscript. This work was supported by National Natural Science Foundation of China (grant number 41902106); State Key Laboratory of Marine Geology, Tongji University (grant number MG201903); State Key Laboratory of Oil and Gas Reservoir Geology and Exploitation (Chengdu University of Technology) (grant number PLC20180301); and China Scholarship Council (grant number 201508510096).

References

Andersen, T., 2002. Correction of common lead in U–Pb analyses that do not report ^{204}Pb. Chem. Geol., 192, 59-79.

Balini, M., Jenks, J.F., Martin, R., McRoberts, C.A., Orchard, M.J., Silberling, N.J., 2015. The Carnian/Norian boundary succession at Berlin-Ichthyosaur State Park (Upper Triassic, central Nevada, USA). Paläontologische Zeitschrift, 89, 399–433.

Balini, M., Krystyn, L., Levera, M., Tripodo, A., 2012. Late Carnian-Early Norian ammonoids from the GSSP candidate section Pizzo Mondello (Sicani Mountains, Sicily). Rivista Italiana di Paleontologia e Stratigrafia (Research In Paleontology and Stratigraphy), 118.

Bernardi, M., Gianolla, P., Petti, F.M., Mietto, P., Benton, M.J., 2018. Dinosaur diversification linked with the Carnian Pluvial Episode. Nat. Commun, 9, 1499.

Dal Corso, J., Benton, M. J., Bernardi, M., Franz, T., Gianolla, P., Hohn, S., Kustatscher, E., Merico, A., Roghi, G., Ruffell, A., Ogg, J. G., Preto, N., Schmidt, A. R., Seyfullah, L. J., Simms, M. J., Shi, Z., Zhang, Y., 2018. First workshop on the Carnian Pluvial Episode (Late Triassic): A report. Albertiana, 44, 49-57.

De Sigoyer, J., Vanderhaeghe, O., Duchêne, S., Billerot, A., 2014. Generation and emplacement of Triassic granitoids within the Songpan Ganze accretionary-orogenic wedge in a context of slab retreat accommodated by tear faulting, Eastern Tibetan plateau, China. J. Asian. Earth. Sci., 88, 192-216.

Deng, K.L., He, L., Qin, D.Y., He, Z.G., 1982. The earlier late Triassic sequence and its sedimentary environment in western Sichuan basin. Oil and Gas Geology, 3, 204-210 (In Chinese with English abstract).

Diakow, L., Orchard, M.J., Friedman, R., 2012. Absolute ages for the Norian Stage: a further contribution from southern British Columbia, Canada. Cordilleran Tectonics Workshop. Geological Association Canada, PacificSection, p. 2.

Dickinson, W.R., Gehrels, G.E., 2009. Use of U-Pb ages of detrital zircons to infer maximum depositional ages of strata: a test against a Colorado Plateau Mesozoic database. Earth. Planet. Sc. Lett., 288, 115-125.

Furin, S., Preto, N., Rigo, M., Roghi, G., Gianolla, P., Crowley, J.L., Bowring, S.A., 2006. High-precision U\Pb zircon age from the Triassic of Italy: implications for the Triassic time scale and the Carnian origin of calcareous nannoplankton and dinosaurs. Geology, 34, 1009-1012.

Gehrels, G.E., Saleeby, J.B., Berg, H.C., 1987. Geology of Annette, Gravina, and Duke Islands, Southeastern Alaska. Can. J. Earth. Sci., 24, 866-881.

Golonka, J., 2007. Late Triassic and early Jurassic palaeogeography of the world. Palaeogeogr. Palaeoclimatol. Palaeoecol., 24., 297-307.

Jiang, H., Yuan, J., Chen, Y., Ogg, J.G., Yan, J., 2019. Synchronous onset of the Mid-Carnian Pluvial Episode in the East and West Tethys: Conodont evidence from Hanwang, Sichuan, South China. Palaeogeogr. Palaeoclimatol. Palaeoecol., 520, 173-180.

Jin, X., Ji, G.F., Shi, Z.Q., Wang, Y.Y., 2015. The sedimentary facies of Guanyinya Section in Hanwang, Mianzhu: implications for the environment evolution ahead of and after the Triassic Carnian Pluvial Event. Geol. Sci. Technol. Info. 34, 1174–1182 (In Chinese with English abstract)

Jin, X., Shi, Z. Q., Rigo, M., Franceschi, M., Preto, N., 2018. Carbonate platform crisis in the Carnian (Late Triassic) of Hanwang (Sichuan Basin, South China): insights from conodonts and stable isotope data. J. Asian. Earth. Sci., 164, 104-124.

Jin, X., McRoberts, A. C., Shi, Z.Q., Mietto, P., Rigo, M., Roghi, G., Manfrin, S., Franceschi, M., Preto, N., 2019. The aftermath of the CPE and the Carnian/Norian transition in northwestern Sichuan Basin, South China. J. Geol. Soc. London., 176, 179-196.

Jin, X., Gianolla, P., Shi, Z., Franceschi, M., Caggiati, M., Du, Y., Preto, N., 2020. Synchronized changes in shallow water carbonate production during the Carnian Pluvial Episode (Late Triassic) throughout Tethys. Glob. Planet. Change., 184, 103035.

Kent, D.V., Olsen, P.E., Mutton, G., 2017. Astrochronostratigraphic polarity time scale (APTS) for the Late Triassic and Early Jurassic from continental sediments and correlation with standard marine stages. Earth. Sci. Rev., 166, 153-180.

Kent, D.V., Olsen, P.E., Rasmussen, C., Lepre, C., Mundil, R., Irmis, R.B., Gehrels, G.E., Giesler, D., Geissman, J.W., Parker, W.G., 2018. Empirical evidence for stability of the 405-kiloyear Jupiter-Venus eccentricity cycle over hundreds of million years. Proc. Natl. Acad. Sci. U.S.A. 6153-6158.

Kent, D.V., Olsen, P.E., Lepre, C., Rasmussen, C., Mundil, R., Gehrels, G.E., Giesler, D., Irmis, R.B., Geissman, J.W., Parker, W.G., 2019.

Magnetochronology of the entire Chinle Formation (Norian age) in a scientific drill core from Petrified Forest National Park (Arizona, USA) and implications for regional and global correlations in the Late Triassic. Geochem. Geophy. Geosy., 20, 4654-4664.

Langer, M. C., Ramezani, J., Da Rosa, Á.A., 2018. U-Pb age constraints on dinosaur rise from south Brazil. Gondwana. Res., 57, 133-140.

Li, Y., Allen, P.A., Densmore, A.L., Qiang, X., 2003. Evolution of the Longmen Shan foreland basin (western Sichuan, China) during the Late Triassic Indosinian orogeny. Basin. Res., 15, 117-138.

Li, Y., Yan, Z., Liu, S., Li, H., Cao, J., Su, D., Dong, S.L., Sun, W., Yang, R.J., Yan, L., 2014. Migration of the carbonate ramp and sponge buildup driven by the orogenic wedge advance in the early stage (Carnian) of the Longmen Shan foreland basin, China. Tectonophysics, 619, 179-193.

Liu, Y., Hu, Z., Zong, K., Gao, C., Gao, S., Xu, J., Chen, H., 2010. Reappraisement and refinement of zircon U-Pb isotope and trace element analyses by LA-ICP-MS. Chinese Sci. Bull., 55, 1535-1546.

Lucas, S.G., Tanner, L.H., Kozur, H.W., Weems, R.E., Heckert, A.B., 2012. The Late Triassic timescale: age and correlation of the Carnian-Norian boundary. Earth. Sci. Rev., 114, 1-18.

Maron, M., Muttoni, G., Rigo, M., Gianolla, P., Kent D.V., 2019. New magneto biostratigraphic results from the Ladinian of the Dolomites and implications for the Triassic geomagnetic polarity timescale. Palaeogeogr. Palaeoclimatol.

Palaeoecol., 517, 52-73.

Mazza, M., Nicora, A., Rigo, M., 2018. Metapolygnathus parvus Kozur, 1972 (Conodonta): a potential primary marker for the Norian GSSP (Upper Triassic). Bollettino della Società Paleontologica Italiana, 57, 81–101.

McRoberts, C.A., Krystyn, L., 2011. The FOD of Halobia austriaca at Black Bear Ridge (northeastern British Columbia) as the base-Norian GSSP, in: Preceedings. Presented at the 21 st Canadian Paleontology Conference, Vancouver, Canada, pp. 38–39.

Muttoni, G., Kent, D.V., Olsen, P.E., Stefano, P.D., Lowrie, W., Bernasconi, S.M., Hernández, F.M., 2004. Tethyan magnetostratigraphy from Pizzo Mondello (Sicily) and correlation to the Late Triassic Newark astrochronological polarity time scale. Geol. Soc. Am. Bull., 116, 1043–1058.

Nicora, A., Balini, M., Bellanca, A., Bertinelli, A., Bowring, S. A., Di Stefano, P., Dumitrica, P., Guaiumi, C., Gullo, M., Hungerbuehler, A., Levera, M., Mazza, M., McRoberts, C.A., Muttoni, G., Preto, N., Rigo, M., 2007. The Carnian/Norian boundary interval at Pizzo Mondello (Sicani Mountains, Sicily) and its bearing for the definition of the GSSP of the Norian Stage. Albertiana, 36, 102-129.

Ogg, J.G., Huang, C., Hinnov, L., 2014. Triassic timescale status: a briefoverview. Albertiana, 41, 3-30.

Orchard, M.J., 2019. The Carnian-Norian boundary GSSP candidate at Black Bear Ridge, British Columbia, Canada: update, correlation, and conodont

taxonomy. Albertiana, 45, 50–68.

Orchard, M.J., 2007. A proposed Carnian-Norian Boundary GSSP at Black Bear Ridge, northeast British Columbia, and a new conodont framework for the boundary interval. Albertiana, 36, 130–141.

Ramezani, J., Hoke, G.D., Fastovsky, D.E., Bowring, S.A., Therrien, F., Dworkin, S.I., Atchley, S.C., Nordt, L.C., 2011. High-precision U\Pb zircon geochronology of the Late Triassic Chinle Formation, Petrified Forest National Park, (Arizona, USA): temporal constraints on the early evolution of dinosaurs. Geol. Soc. Am. Bull., 123, 2142-2153.

Reimink, J.R., Davies, J.H., Waldron, J.W., Rojas, X., 2016. Dealing with discordance: a novel approach for analysing U-Pb detrital zircon datasets. J. Geol. Soc. London.,173, 577-585.

Rigo, M., Preto, N., Francesconi, M., Guaiumi, C., 2012. Stratigraphy of the Carnian-Norian Calcari con Selce Formation in the Lagonegro Basin, Southern Apennines. Rivista Italiana di Paleontologia e Stratigrafia, 118, 143-154.

Rigo, M., Mazza, M., Karádi, V., Nicora, A., 2018. New Upper Triassic Conodont Biozonation of the Tethyan Realm. In: Tanner L. (eds) The Late Triassic World. Topics in Geobiology, vol 46. Springer, Cham.

Salvador, A., 1994. International Stratigraphic Guide: A Guide to Stratigraphic Classification, Terminology, and Procedure. Geological Society of America, 248 pp.

Sláma, J., Košler, J., Condon, D.J., Crowley, J.L., Gerdes, A., Hanchar, J.M.,

Horstwood, M.S.A., Morris, G.A., Nasdala, L., Norberg, N., Schaltegger, U., Schoene, B., Tubrett, M.N., Whitehouse, M.J., 2008. Plešovice zircon — a new natural reference material for U–Pb and Hf isotopic microanalysis. Chem. Geol., 249, 1-35.

Schoene, B. 2014. U-Th-Pb geochronology. In: Holland, H.D. Turekian, K.K. (eds) The Crust. Treatise on Geochemistry, 4, 2nd edn. Elsevier, Oxford, 341-378.

Shao, T., Cheng, N., Song, M., 2016. Provenance and tectonic-paleogeographic evolution: Constraints from detrital zircon U–Pb ages of Late Triassic-Early Jurassic deposits in the northern Sichuan basin, central China. J. Asian. Earth. Sci., 127, 12-31.

Shi, Z.Q, Preto, N., Jiang, H.S, Krystyn, L., Zhang, Y., Ogg, J.G., Jin, X., Yuan, J.L., Yang, X.K., Du, Y.X., 2017. Demise of Late Triassic sponge mounds along the northwestern margin of the Yangtze Block, South China: Related to the Carnian Pluvial Phase? Palaeogeogr. Palaeoclimatol. Palaeoecol., 474, 247-263.

Shi, Z.Q., Jin. X., Preto. N., Rigo, M., Du, Y.X., Han, L., 2019. The Carnian Pluvial Episode at Ma'antang, Jiangyou in Upper Yangtze Block, Southwestern China. J. Geol. Soc. Lond., 176, 197-207.

Shi, Z.S, Guo, C.M., 2019. Facies model of a mixed siliciclastic-carbonate ramp of the Ma'antang Formation (Carnian period), Sichuan Basin, China. Arab. J. Geosci., 12, 725.

Simms, M.J., Ruffell, A.H., 1989. Synchroneity of climatic change and extinctions

in the Late Triassic. Geology, 17, 265.

Spencer, C.J., Kirkland, C.L., Taylor, R.J., 2016. Strategies towards statistically robust interpretations of in situ U-Pb zircon geochronology. Geosci. Front., 7, 581-589.

Tozer, E.T., 1994. Canadian Triassic ammonoid faunas. Geol. Surv. Can. Bull., 467, 1-663.

Wang, Y.S., 1992. The earlier late Triassic ammonties from Longmen Mountains. J. Chengdu. Colleg. Geol, 19, 28-35. (In Chinese with English Abstract).

Weislogel, A.L, Graham, S.A, Chang, E.Z, Wooden, J.L, Gehrels, G.E, Yang, H., 2006. Detrital zircon provenance of the Late Triassic SongpanGanzi complex: Sedimentary record of collision of the North and South China Blocks. Geology, 34, 97-100

Weislogel, A.L., 2008. Tectonostratigraphic and geochronologic constraints on evolution of the northeast Paleo-Tethys from the songpan-ganzi complex, central china. Tectonophysics, 451, 0-345.

Wiedenbeck, M., Alle, P., Corfu, F., Griffin, W.L., Meier, M., Oberli, F., Von Quadt, A., Roddick, J.C., Spiegel, W., 1995. Three natural zircon standards for U-Th-Pb, Lu-Hf, trace element and REE analyses. Geostandards Newsletter, 19, 1-24.

Wu, X., 1984. Paleoecological characteristics of Late Triassic sponge patch reefs in northwestern Sichuan. China. J. Chengdu. Colleg. Geol, 43-54. (In Chinese with English Abstract).

Wu, X., 1989. Carnian (upper triassic) sponge mounds of the Northwestern Sichuan Basin, China: Stratigraphy, facies and paleoecology. Facies, 21, 171-187.

Wu, X., 2009. Sedimentary facies analysis of the Late Triassic Carnian siliceous sponge reef-oolitic bank complex in northwestern Sichuan province. J. Palaeogeogr, 11, 125-142. (In Chinese with English Abstract).

Zhang, G., Meng, Q., Yu, Z., Sun, Y., Zhou, D., Guo, A., 1996. Orogenesis and dynamics of the Qinling orogen. Science in China Series D-Earth Sciences, 39, 225-234. (In Chinese with English Abstract)

Zhang, Y., Li, M.S., Ogg, J.G., Montgomery, P., Huang, C., Chen, Z.Q., Shi, Z.Q., Enos, P., Lehrmann, D.J., 2015. Cycle-calibrated magnetostratigraphy of middle Carnian from south China: Implications for Late Triassic time scale and termination of the Yangtze platform. Palaeogeogr. Palaeoclimatol. Palaeoecol., 436, 135-166.

Figure captions

Fig. 1. A) General position of the NW Sichuan Basin during the Late Triassic period (simplified from Golonka, 2007). S. China: South China Block; N. China: North China Block. **B)** Geological and tectonic map of the Sichuan Basin and its link to adjacent areas (simplified from Li et al., 2003); **C)** Geological map showing the locations of Qingyangou (HWQ) and Jushui (JS) sections (simplified from Wu, 1989). The topographic map of the Hanwang and Jushui towns on the top left corner are taken from Google Earth. J: Jurassic; P: Permian; T_1: Lower Triassic; T_2: Middle

Triassic; T_{3m}: Ma'antang Formation (Upper Triassic); T_{3x}: Xujiahe Formation (Upper Triassic); Q: Quaternary.

Fig. 2. The lithology, zircon sampling position and biostratigraphic correlation of Qingyangou (HWQ) section and Jushui (JS) section. The ammonoids, conodonts, bivalves and palynological assemblage zones are from previous studies (Jin et al., 2018, 2019). The ammonoids Discotropitid n. sp. and Juvavitid? are from the JS section based on the studies of Shi Z-Q et al.(2017). The new ammonoid names (this study), *Sinotropites sichuanensis* n. sp. and *Hadrothisbites jushuiensis* sp.n., refer to the old ammonoid names, Tropitid n. gen. n. sp. and *Hadrothisbites*. n. sp., illustrated in Jin et al. (2019), respectively. Pa: palynomorphs, Bi: bivalves, Conos: conodonts, "W" = wackestone, "P/G" = packstone grainstone, "F" = floatstone, "B" = boundstone. DKC: *Dictyophyllidites-Kyrtomisporis-Canalizonospora* assemblage. "Tjs" = Tianjingshan Fomation. Letters besides ammonoids (A-H) are fossiliferous horizons used in the text.

Fig. 3. A). Representative cathodoluminescence (CL) images of detrital zircons from the northwestern Sichuan Basin. The young zircons mainly showing prismatic or euhedral morphology. The analytical spots marked as red circles. **B**).Concordia plots for zircons grains from sample ZQ. **C**). Probability density distribution curves of detrital zircon ages of sample ZQ in the Qingyangou (HWQ) section. **D**). Concordia plots of youngest zircons of sample ZQ. **E**). The weighted mean age of the youngest zircons (n=12).

Fig. 4. Reported U-Pb ages which are comparable with biostratigraphy across the

Carnian/Norian boundary. The ages for the top of Norian (~209.5 Ma) and base of the Carnian (~237.0 Ma) based on the "Short-Tuvalian" option of Ogg et al. (2014). The age of the Carnian/Norian boundary (dashed line) was anchored at ~227.0 Ma based on Kent et al. (2017). The geological time scale of Julian-Tuvalian followed Bernardi et al. (2018) and of Lacian to Sevatian followed Rigo et al. (2018). SE Alaska (225 ± 3 Ma, Gehrels et al., 1987), Southern Italy (230.91 ± 0.33 Ma, Furin et al., 2006), Southern British Columbia (223.8 ± 0.74 Ma and 224.47 ± 0.29 Ma, Daikow et al., 2012). NW Sichuan Basin (227.2 ± 1.1 Ma, this study).

Fig. A. 1. Type species. *Sinotropites sichuanensis* n. sp. (Jin et al., 2019) from the HWQ and JS sections. **A/B)** specimen MGP-PD 31989, internal mold with parts of the shell preserved, position G of the JS section (Fig. 2). **C)** specimen MGP-PD 31978, internal mold, position B of the HWQ section.

Fig. A. 2. Type species. *Sinotropites sichuanensis* n. sp. (Jin et al., 2019) from the HWQ section. **A)** specimen MGP-PD 31970, external mold, position A. **B)** specimen MGP-PD 31976, internal mold, position A. **C)** specimen MGP-PD 31981, external and internal mold, position C. **D)** specimen MGP-PD 31973, internal mold with parts of the shell, position B. **E)** specimen MGP-PD 31977, internal mold, position B. **F)** specimen MGP-PD 31971, internal mold, position A. **G)** specimen MGP-PD 31982, external mold with parts of the shell, position D. **H)** specimen MGP-PD 31975, internal mold, position B. **I)** specimen MGP-PD 31975, external mold, position B. **J)** specimen MGP-PD 31974, internal mold, position B.

Fig. A. 3. Type species. *Sinotropites sichuanensis* n. sp. (Jin et al., 2019) from the JS

section. **A)** specimen MGP-PD 31987, internal mold, position G. **B)** specimen MGP-PD 31984, internal mold, position F. **C)** specimen MGP-PD 31992, internal mold, position H. **D)** specimen MGP-PD 31991, with shell preserved, position H. **E)** specimen MGP-PD 31985, external and internal mold, position G. **F)** specimen MGP-PD 31990, internal mold with parts of shell, position H. **G)** specimen MGP-PD 31983, internal mold, position F. **H)** specimen MGP-PD 31986, internal mold with parts of shell, position G. **I)** specimen MGP-PD 31993, internal mold with parts of shell, position H.

Fig. A. 4. *Hadrothisbites jushuiensis* sp.n. (Jin et al., 2019) from the JS section. MGP-PD 31988, internal and external mold, and parts of shell, position G of the JS section (Fig. 2).

Appendix. Systematic descriptions

Order Ceratitida Hyatt, 1884

Superfamily Tropitoidea Mojsisovics, 1875

Family Tropitidae Mojsisovics, 1875

Sinotropites gen. n.

Derivio nominis: With reference to the occurrence from China.

Type species: *Sinotropites sichuanensis* n. sp. (for monotype), Fig. A.1/A, B, C.

Diagnosis: Tropitidae characterized by keel without ventral sulci and subrectangular to subovoidal whorl section. The flank bears ribs without nodes.

Description: The type species presents involute and compressed shell, with the

coiling that increases in height during growth. The phragmocone shows a subrectangular whorl section at first that becomes subovoidal later on. The umbilical area shows a slightly angular rim and a steep umbilical wall. The venter is characterized by a distinct rounded keel in all ontogenetic stages, without ventral sulci.

Remarks: The new genus *Sinotropites* shows morphological similarities with *Discotropites* Hyatt & Smith, 1905. Nevertheless, the latter genus chiefly differs by having ventral sulci bordering the ventral keel, trigonal whorl section during ontogeny and ribs quite broader respect the interspaces.

Occurrence and age: At present, the new genus has been found in the uppermost Carnian (uppermost Tuvalian: *Anatropites spinosus* Zone, *Gonionotites italicus* Subzone) of the Ma'antang Formation cropping out in the Qingyangou and Jushui sections (Sichuan region, China).

Sinotropites sichuanensis sp. n.

(Fig. A.1/A, B, C; Fig. A.2/A, B, C, D, E, F, G, H, I, J; Fig. A.3/A, B, C, D, E, F, G, H, I)

Derivatio nominis: From Sichuan region (China).

Stratum typicus and locus typicus. Position B of the Qingyangou section (Fig. 2).

Type series: Holotype MGP-PD 31973 (D), Fig. A.2; Paratypes MGP-PD 31977 (E), Fig. A.2; MGP-PD 31984 (E), Fig. A.3; MGP-PD 31985 (H), Fig. A.3; MGP-PD 31991 (I), Fig. A.3.

Material: HWQ section A (MGP-PD 31970), F (MGP-PD 31971), D (MGP-PD

31973), J (MGP-PD 31974), H/I (MGP-PD 31975), B (MGP-PD 31976), E (MGP-PD 31977), C (MGP-PD 31981), J (MGP-PD 31982). All are illustrated in Fig. A.2. C (MGP-PD 31978), Fig. A.1. JS section G (MGP-PD 31983), B (MGP-PD 31984), E (MGP-PD 31985), H (MGP.PD 31986), A (MGP-PD 31987), F (MGP-PD 31990), D (MGP-PD 31991), C (MGP-PD 31992), I (MGP.PD 31993). All are illustrated in Fig. A.3. A/B (MGP-PD 31989), Fig. A.1.

Diagnosis: *Sinotropites* characterized by thin sigmoid ribs showing swellings at the ventrolateral margin that fade during ontogenesis. In early growth stages, the ribs are sharply rounded in section, less wide respect the interspaces, even if the test is preserved.

Description: Involute and compressed shell, with the coiling that increases in height during growth. The phragmocone shows a subrectangular whorl section at first then subovoidal later on. The umbilical area shows a slightly angular rim and a steep umbilical wall. The venter is characterized by a distinct rounded keel in all ontogenetic stages, without ventral sulci. At first, the ornamentation of the flank consists by sigmoid ribs, sharply rounded in section, less broad respect the interspaces, even if the shell is provided with test. During growth the ribs are markedly projected and as broad as the interspaces if the test is preserved. Along the flank primary, simple ribs generally occur. Infrequent ribs joined in pairs at the umbilical rim are present. In early growth stages the ribs are slightly broader towards the outer part of the flank where appear as elongated swellings. No nodes are present. At small whorl height (about 4 mm) the suture line suggests an ammonitic outline

characterized by three tapered saddles with the first lateral lobe broad and deeply indented. Crenulations can be observed on the first and second lateral saddles (Fig. A. 1). It must be pointed out that the suture lines are taken at a small diameter, and they may be far to be fully developed, so that the ammonitic outline could become even more obvious during ontogeny.

Dimensions (mm).

	D	H	h	U	W	w	H/D	U/D	SGP
Fig. A.2/B, D (holotype)	12	5.6	3.9	2.5	4.8	x	0.46	0.20	43.6
Fig. A.2/E (paratype 1)		6.5		5.3					
Fig. A.3/E (paratype 2)		5.5							
Fig. A.3/H (paratype 3)	13.4	6.1	4.3	3	0.45	0.22	41.9		
Fig. A.3/I (paratype 4)	12	5.6	3.9	2.5	0.46	0.20	43.6		

Remarks: For its morphological features the new species is not comparable with any other taxon so far described.

Occurrence and age. At present, the new species has been found in the uppermost Carnian (uppermost Tuvalian: *Anatropites spinosus* Zone, *Gonionotites italicus* Subzone) of the Ma'antang Formation cropping out in the Qingyangou and Jushui sections (Sichuan region, China). In Position A of the Qingyangou section, *Sinotropites sichuanensis* sp. n. occurs along with *Gonionotites* sp.. *Gonionotites* is a Carnian genus, which distribution continue into the lower Norian (e.g., Tozer, 1994; Balini et al., 2012, 2015). Conodonts of the Qingyangou section are late Carnian, and occur only 2-3 m below the ammonoids. Magnetostratigraphy is available for the

Qingyangou section (Zhang et al., 2015). Sample Position A, which yielded *Gonionotites* sp. and *Sinotropites sichuanensis* sp. n., corresponds to a reverse polarity interval that may be correlated either to Carnian beds or to the interval of uncertain age in the Tethyan Pizzo Mondello section, which is being considered as a candidate for the Norian GSSP (e.g., Balini et al., 2015). For these reasons, *Sinotropites sichuanensis* sp. n. is here considered a Carnian species. This age attribution may change, as better correlations with the Tethyan Triassic become available and a formal definition of the Norian stage is being achieved. Tropitidae did not survive into the Norian, and this so far holds also for *Sinotropites sichuanensis* sp. n.

Family Thisbitidae Spath, 1951

Hadrothisbites jushuiensis sp.n.

(Fig. A.4)

Derivatio nominis: With reference to the occurrence from the Jushui section (Sichuan region, China), where the new taxon was found.

Stratum typicus and locus typicus. Position G of the Jushui section.

Type series: Holotype MGP-PD 31988, see Fig. A.4.

Material: Only the holotype.

Diagnosis: Thisbitid characterized by thin, numerous, randomly arranged ribs in the inner whorls but with smooth body chamber.

Description: The unique specimen at disposal shows a crushed but not deformed shell partially included in the matrix. Despite that, the morphological features are so unique to avoid any confusion with previous taxa.

The shell shows a slight increasing in height of the whorl which is subrectangular in section. The last whorl slightly embraces the previous one. The venter is flat and marked by a median keel. The phragmocone is characterized by quite thin, numerous, fairly sigmoid ribs. On the flank primary, periumbilical bifurcated and intercalatory ribs are randomly alternated. In the body chamber or just before this ribs framework disappear. Only indistinct ribs occur in the outer third of the flank in the adapical part of the body chamber. As for the nodes, they are rounded, regularly spaced and present only in the external margin.

In the inner part of the shell, which is visible in crushed parts, a portion of the suture line is inferred, showing a ceratitic outline in which a first broad entire lateral saddle is visible.

Dimensions (mm).

	D	H	h	U	W	w	H/D	U/D	SGR
Fig. A.4 (holotype)	16,3	6,7	4,4	5,2	0,41	0,32	52,3		

Remark: *Hadrothisbites* was originally defined as a monospecic genus, characterized by a finely ornamented shell in which the body chamber shows thin, regularly looped ribs and external nodes of variable strength (Tozer, 1994). The new species exhibits a smooth body chamber bordered, in the ventrolateral margin, by a row of rounded regularly spaced nodes. Albeit somehow different from the original description, we find the quoted species similar enough to attribute it to the genus *Hadrothisbites*. The resemblances of the phragmocone ribs framework, the sharp carinate venter, the inferred whorl section outline and the evolution degree of the shell are in fact

consistent. For the morphological differences of the body chamber, *Hadrothisbites jushuiensis* sp.n. cannot be confused with *Hadrothisbites taylori* Tozer, 1994, type species of the genus.

Occurrence and Age. At present, the new species has been found in the uppermost Carnian (uppermost Tuvalian: *Anatropites spinosus* Zone, *Gonionotites italicus* Subzone) of the Ma'antang Formation cropping out in the Jushui section (Sichuan region, China), coexisting in the same bed with *Sinotropites sichuanensis* gen.n., sp.n.

Declaration of interests

☐ The authors declare that they have no known competing financial interests or personal relationships that could have appeared to influence the work reported in this paper.

☐The authors declare the following financial interests/personal relationships which may be considered as potential competing interests:

The authors declare that they have no known competing financial interests or personal relationships that could have appeared to influence the work reported in this paper.

Highlights:

1. We report a U/Pb age of 227.2 ± 1.1 Ma associated with ammonoids in South China.
2. *Sinotropites sichuanensis* and *Hadrothisbites jushuiensis* are described in Sichuan.
3. The terrigenous turnover in Hanwang and Jushui area is not related to the CPE.

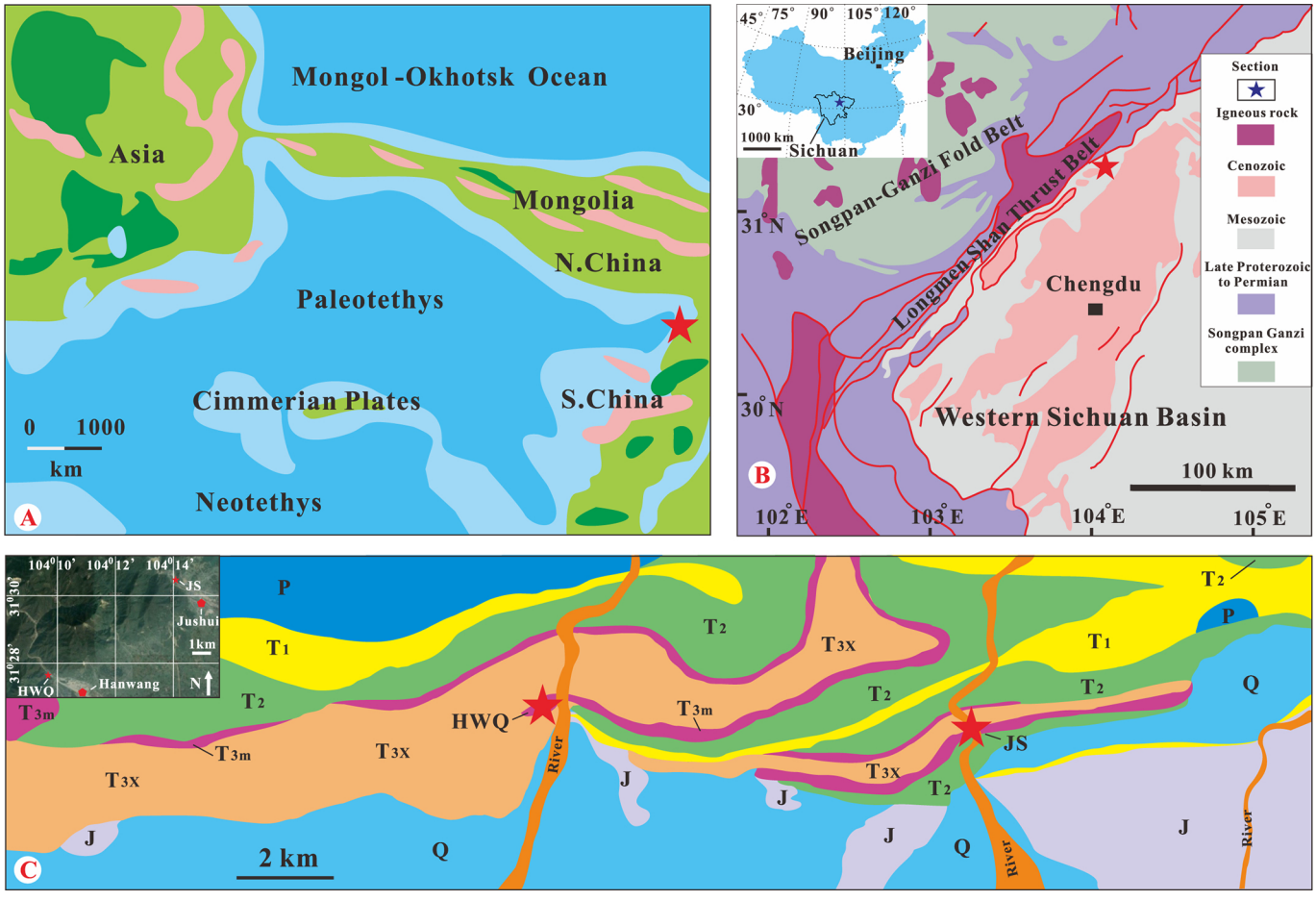
Mongol-Okhotsk Ocean
Asia
Mongolia
N.China
Paleotethys
Cimmerian Plates
S.China
0 1000
km
Neotethys
A
45° 75° 90° 105° 120°
30°
Beijing
1000 km
Sichuan
Songpan-Ganzi Fold Belt
Longmen Shan Thrust Belt
31°N
30°N
Chengdu
Western Sichuan Basin
100 km
102°E
103°E
104°E
105°E
B
Section
Igneous rock
Cenozoic
Mesozoic
Late Proterozoic to Permian
Songpan Ganzi complex
104°10' 104°12' 104°14'
31°30'
31°28'
JS
Jushui
1km
HWQ
Hanwang
N
P
T1
T2
T3m
T3x
J
Q
River
2 km
C

Figure 1

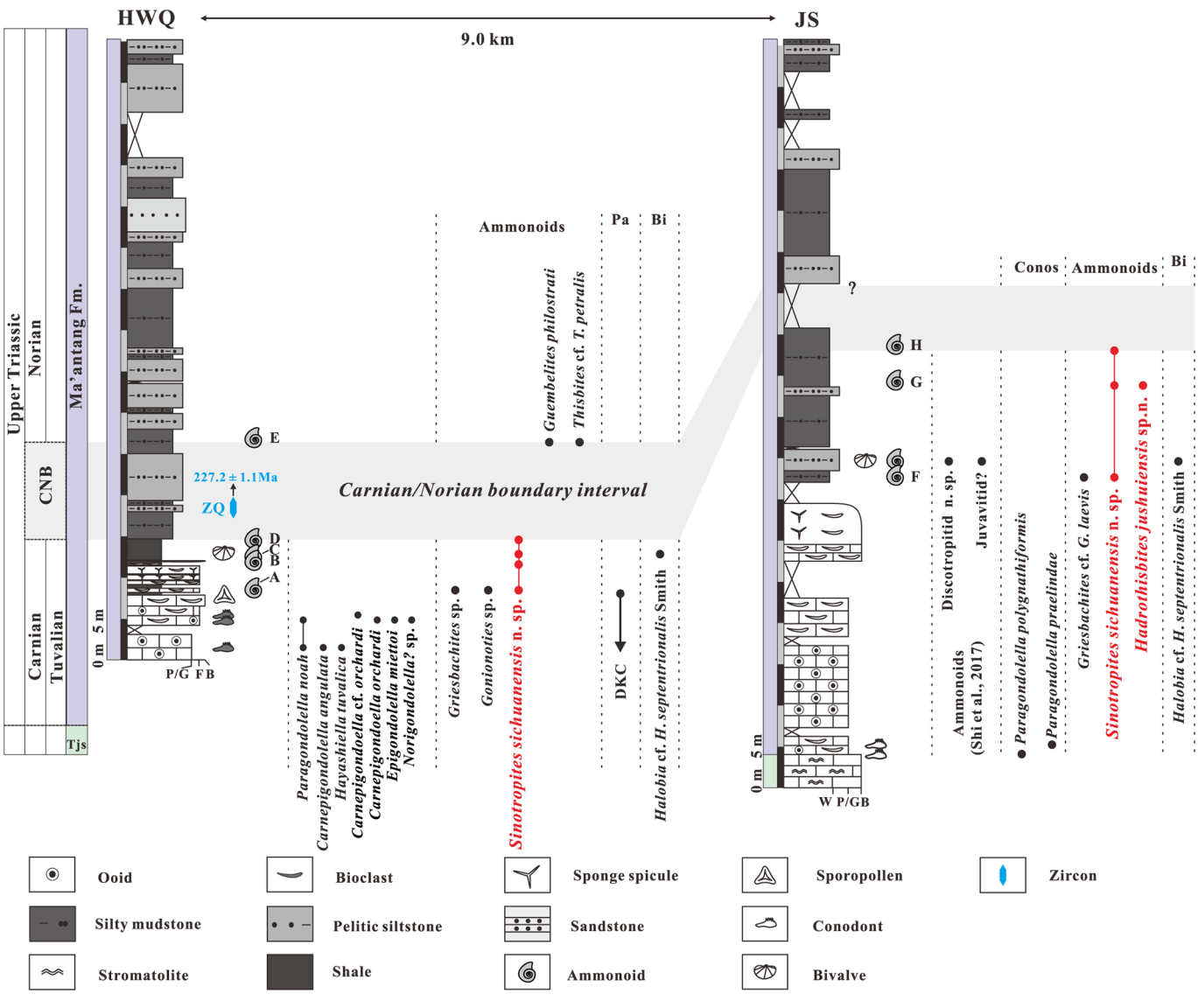
HWQ
9.0 km
JS
Upper Triassic
Norian
Carnian
Tuvalian
CNB
Ma'antang Fm.
Tjs
Ammonoids
Pa
Bi
Guembelites philostrati
Thisbites cf. T. petralis
E
227.2 ± 1.1Ma
ZQ
Carnian/Norian boundary interval
D
C
B
A
0 m 5 m
P/G F B
Griesbachites sp.
Gonionoties sp.
Sinotropites sichuanensis n. sp.
DKC
Halobia cf. H. septentrionalis Smith
Paragondolella noah
Carnepigondolella angulata
Hayashiella tuvalica
Carnepigondoella cf. orchardi
Carnepigondoella orchardi
Epigondolella miettoi
Norigondolella? sp.
?
H
G
F
Conos
Ammonoids
Bi
Discotropitid n. sp.
Ammonoids (Shi et al., 2017)
Juvavitid?
Paragondolella polygnathiformis
Paragondolella praelindae
Griesbachites cf. G. laevis
Sinotropites sichuanensis n. sp.
Hadrothisbites jushuiensis sp.n.
Halobia cf. H. septentrionalis Smith
0 m 5 m
W P/GB
Ooid
Silty mudstone
Stromatolite
Bioclast
Pelitic siltstone
Shale
Sponge spicule
Sandstone
Ammonoid
Sporopollen
Conodont
Bivalve
Zircon

Figure 2

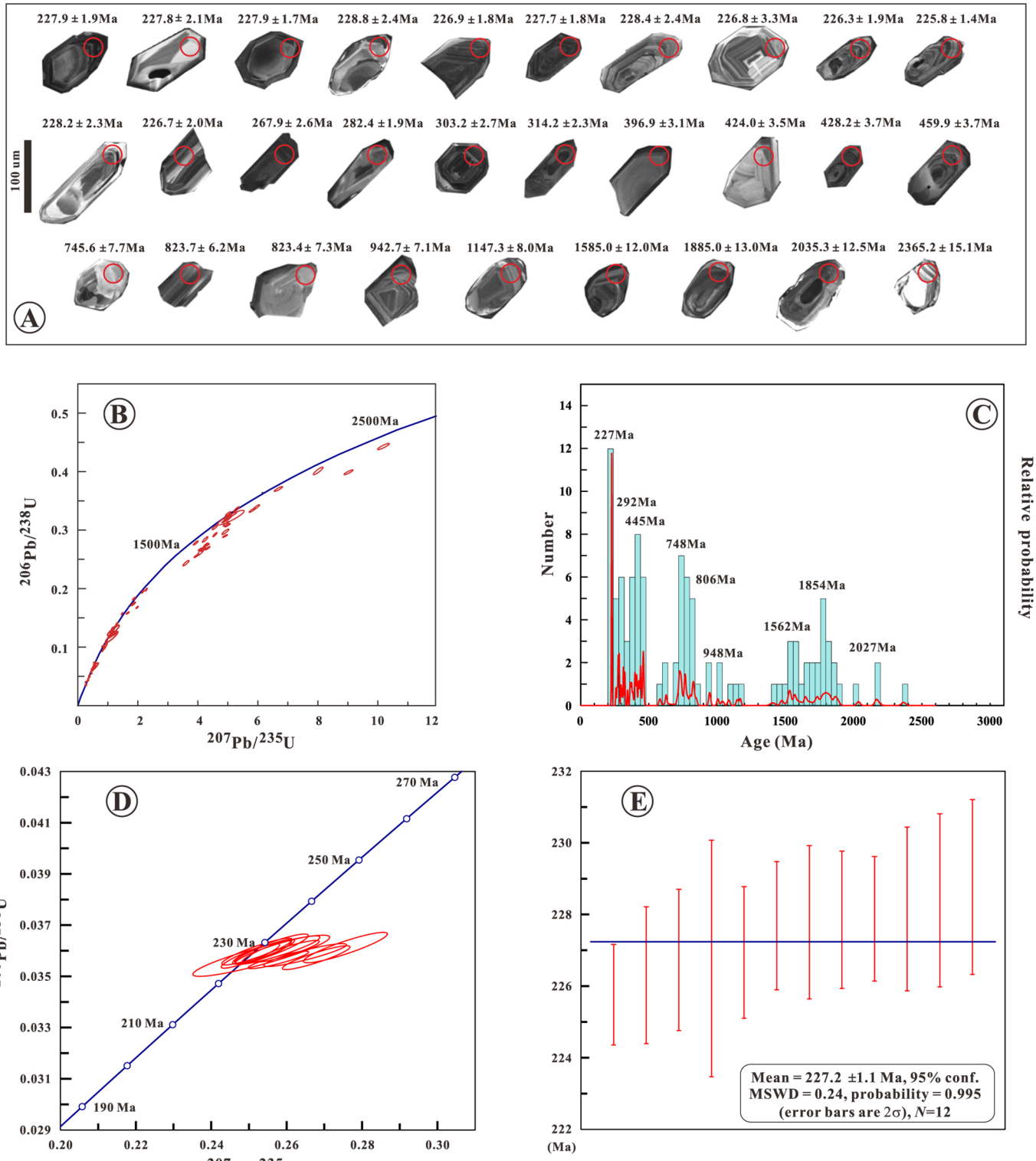
A
227.9 ± 1.9Ma
227.8± 2.1Ma
227.9 ± 1.7Ma
228.8 ± 2.4Ma
226.9 ± 1.8Ma
227.7 ± 1.8Ma
228.4 ± 2.4Ma
226.8 ± 3.3Ma
226.3± 1.9Ma
225.8 ± 1.4Ma
228.2 ± 2.3Ma
226.7± 2.0Ma
267.9± 2.6Ma
282.4 ±1.9Ma
303.2 ±2.7Ma
314.2 ±2.3Ma
396.9 ±3.1Ma
424.0± 3.5Ma
428.2± 3.7Ma
459.9 ±3.7Ma
100 um
745.6 ±7.7Ma
823.7± 6.2Ma
823.4± 7.3Ma
942.7± 7.1Ma
1147.3 ± 8.0Ma
1585.0 ± 12.0Ma
1885.0 ± 13.0Ma
2035.3 ± 12.5Ma
2365.2 ± 15.1Ma
B
2500Ma
1500Ma
206Pb/238U
207Pb/235U
C
227Ma
292Ma
445Ma
748Ma
806Ma
948Ma
1562Ma
1854Ma
2027Ma
Number
Age (Ma)
Relative probability
D
270 Ma
250 Ma
230 Ma
210 Ma
190 Ma
206Pb/238U
207Pb/235U
E
Mean = 227.2 ±1.1 Ma, 95% conf.
MSWD = 0.24, probability = 0.995
(error bars are 2σ), N=12
(Ma)

Figure 3

Epoch
Stage
Sub-stage
Upper Triassic
Norian
Carnian
Sevatian
Alaunian
Lacian
Tuvalian
Julian
~ 209.5 Ma
~ 227.0 Ma
~ 237.0 Ma
SE Alaska
Southern Italy
Southern British Columbia
NW Sichuan

Figure 4